

Adiabatic approximation for linear and nonlinear lambda and tripod systems with losses

Viktoras Pyragas^{1,2} and Gediminas Juzeliunas¹

¹*Institute of Theoretical Physics and Astronomy of Vilnius University, LT-01108 Vilnius, Lithuania*

²*Semiconductor Physics Institute of Center for Physical Sciences and Technology, LT-01108 Vilnius, Lithuania*

(Dated: March 22, 2019)

We present the stability analysis of the dark states in the adiabatic passage for the linear and nonlinear lambda and tripod systems. For the linear systems, using the basis comprising bright, excited and dark states the first two states can be adiabatically eliminated. Subsequently the system evolves in the 1D (the lambda system) or 2D (the tripod system) Hilbert subspaces. The validity of such approximations is confirmed by an analytic evaluation of the real parts of eigenvalues of the corresponding Jacobians, the non-zero eigenvalues of which are found from quadratic characteristic equations, as well as by the corresponding numerical simulations. The number of negative real parts dictates the number of variables that can be adiabatically eliminated. The number of zero real parts yields the dimensionality of the remaining system. In the cases of nonlinear systems, we evaluate the Jacobians at the dark states. Similarly to the linear systems, here we also find the non-zero eigenvalues from the characteristic quadratic equations. A distinctive feature of nonlinear systems is the absence of the principle of superposition making the stability analysis more complex.

PACS numbers: 42.50.Ct

I. INTRODUCTION

Over the last couple of decades there has been a continuing interest in the stimulated Raman adiabatic passage (STIRAP) [1–5]. The simplest situation is the adiabatic passage in a linear lambda system [6–12] containing a single dark (uncoupled) state which is immune to the atom-light coupling. If atomic initial and final states are the ground states representing the dark states of the system, the atom can be transferred between these two states by slowly changing the relative intensity of the laser pulses. When the adiabatic passage is slow enough, the excited state is only slightly populated and thus the losses are minimum. The analysis has been extended for the STIRAP process in the tripod system characterized by two dark states [13–15]. This enables to create a quantum superposition of metastable states out of a single initial state in a robust and coherent way [16, 17]. The schemes involving more atomic and molecular levels were also proposed for creation a superposition of states [18] as well as for experimental control of excitation flow [19]. Recently the treatment was further extended to the nonlinear lambda [20–31] and tripod [32] schemes.

The aim of the present work is to perform a stability analysis of the dark states in the adiabatic passage for the linear and nonlinear lambda and tripod systems. The analysis sets limits to the adiabatic reduction of the considered systems. Although the linear lambda [1–12] and tripod systems [13–17, 33] have been substantially studied in the literature, here we apply our treatment to these linear setups as well in order to facilitate the subsequent analysis of the non-linear systems.

The nonlinear tripod system can be realized in the photoassociation (PA) with two target states involved. It was first considered in Ref.[32] in which the second order dynamic system was derived that parametrizes the solu-

tion evolving on the dark state manifold. However the stability of the solution moving along the manifold was not considered. Therefore we shall check the stability of this solution, i.e. see whether the nearby solutions are attracted back to this manifold.

In the optical photoassociation the STIRAP can be an efficient way to create the ground-state molecules by taking an advantage of dark states [20, 21]. Yet, differently from the traditional STIRAP in an atomic lambda system, the atom-molecule STIRAP contains nonlinearities originating from the conversion process of atoms to molecules, as well as from the interparticle interactions described by the non-linear mean-field contributions. The existence of such nonlinearities makes it difficult to analyze the adiabaticity of the atom-molecule conversion systems due to the absence of the superposition principle. In the STIRAP, the linear instability could make the quantum evolution deviate from the dark state rapidly even in adiabatic limit [22]. Therefore, it is important to avoid such an instability for the efficiency of the STIRAP.

The adiabatic theory for nonlinear quantum systems was first discussed by Liu *et al.* [34] who obtained the adiabatic conditions and adiabatic invariants by representing the nonlinear Heisenberg equation in terms of an effective classical Hamiltonian. Pu *et al.* [23] and Ling *et al.* [24] extended such an adiabatic theory to the atom-dimer conversion system by linking the nonadiabaticity with the population growth in the collective excitations of the dark state. Specifically, it was shown that a passage is adiabatic if the solution remains in a close proximity to the dark state. Itin and Watanabe [25] presented an improved adiabatic condition by applying methods of the classical Hamiltonian dynamics. The atom-molecule dark-state technique in the STIRAP was theoretically generalized to create more complex homonuclear or het-

eronuclear molecule trimers or tetramers [35–38].

An important issue is the instability and the adiabatic property of the dark state in such complex systems. For example, the dynamics of a nonlinear lambda system describing Bose-Einstein condensates (BEC) of atoms and diatomic molecules was studied and a model of the dark state with collisional interactions was investigated [26, 27]. It was shown that nonlinear instabilities can be used for precise determination of the scattering lengths. On the other hand, the transfer of atoms to molecules via STIRAP is robust with respect to detunings, χ^3 nonlinearities, and small asymmetries between the peak strengths of the two Raman lasers [27]. The complete conversion is destroyed by spatial effects unless the time scale of the coupling is much faster than the pulse duration. In addition, a set of robust and efficient techniques has been introduced [39] to coherently manipulate and transport neutral atoms based on three-level atom optics (TLAO).

It is to be noted that the dynamics of an adiabatic sweep through a Feshbach resonance was studied [40] in a quantum gas of fermionic atoms. An interesting application of BEC is an atom diode with a directed motion of atoms [41]. Another example of BEC was presented in Ref. [42] where it was shown that the two-color PA of fermionic atoms into bosonic molecules via a dark-state transition results in a significant reduction of the group velocity of the photoassociation field. This is similar to the Electromagnetically induced transparency (EIT) in atomic systems characterized by the three-levels of the lambda type. In addition the coupled nonlinear Schroedinger equations have been considered [43] to describe the atomic BECs interacting with the molecular condensates through the STIRAP loaded in an external potential. The results have shown that there is a class of external potentials where the exact dark solutions can be formed.

A relevant tool for studying the adiabaticity is the adiabatic fidelity. It indicates how far is the current solution of the system from the dark state. Meng *et al.* have generalized the definition of fidelity for the nonlinear system [28]. They have studied the dynamics and adiabaticity of the population transfer for atom-molecule three-level lambda system on a STIRAP. It was also discussed how to achieve higher adiabatic fidelity for the dark state through optimizing the external parameters of the STIRAP. In the subsequent paper [44] Meng *et al.* have used the same definition of adiabatic fidelity in order to discuss the adiabatic evolution of the dark state in a nonlinear atom-trimer conversion due to a STIRAP. It is to be noted that Ivanov and Vitanov have recently proposed novel high-fidelity composite pulses for the most important single-qubit operations [45].

In this work, we analyze the problem of reducing the dimension (simplifying) in the linear/nonlinear three- and four-level models. The procedure of reduction is called the adiabatic approximation, and its validity is closely related with the theory of adiabaticity discussed above.

The exact three- or four-level system may be adiabatically reduced to a system with lower dimension. The question that arises is how many dynamic variables can be eliminated? In other words, what is the effective dimension of the system? The answer lies in the eigenvalues of the Jacobian computed at the dark state. The zero real parts of eigenvalues mean that in some directions the nearby solutions are behaving neutrally in respect to the dark state. The negative real parts in turn mean that some directions are stable, and the nearby solutions converge towards the dark state. Therefore we conclude that the number of negative real parts dictates the number of variables that can be adiabatically eliminated (see e.g. Ref.[46]). On the other hand, the number of zero real parts yields the effective dimension of the system. Note that we find the non-zero eigenvalues analytically from quadratic characteristic equations.

One of the central issues in our work is the presence of dissipation in all the considered systems. The non-zero losses make the adiabatic approximation easier to implement since the term of losses acts as a "controller" that attracts the nearby solutions towards the dark state. However, Vitanov and Stenholm have demonstrated that the losses cause also the decrease of transfer efficiency to the target state [8]. This decrease can be circumvented by higher pulse areas since the range of decay rates over which the transfer efficiency remains high, has been found to be proportional to the squared pulse area (see Eq.(10) in [8]). In the subsequent developments the effect of spontaneous emission on the population transfer efficiency in STIRAP was explored for the linear lambda [10, 11] and tripod [15] systems. On the other hand, here we concentrate on the stability issues of the linear and non-linear lambda and tripod systems with the losses.

The paper is organized as follows. In next two Sections we shall consider the stability of the linear lambda and tripod systems with losses. In Sections IV and V the analysis is extended to the nonlinear lambda and tripod systems. In Sec.VI we discuss the role of the one-photon detuning followed by the conclusions in Sec.VII.

II. THE LINEAR LAMBDA SYSTEM

In this Section we shall provide a summary on the STIRAP in the linear lambda system with losses studied in Refs.[8, 10, 11] followed by the stability analysis of the system. The three-level lambda system is shown in Fig.1. The excited state $|e\rangle$ is coupled to two ground states $|a\rangle$ and $|g\rangle$ with the coupling strengths denoted as Ω_p and Ω_d to form a lambda scheme. The Hamiltonian of such system reads:

$$H = -\hbar(\Delta + i\gamma)|e\rangle\langle e| + \frac{\hbar}{2}[\Omega_p|a\rangle\langle e| + \Omega_d|g\rangle\langle e| + H.c.]. \quad (1)$$

Note that in this Hamiltonian the one-photon detuning is complex-valued. Its imaginary part represents the losses. Denoting the amplitudes of the three-level state

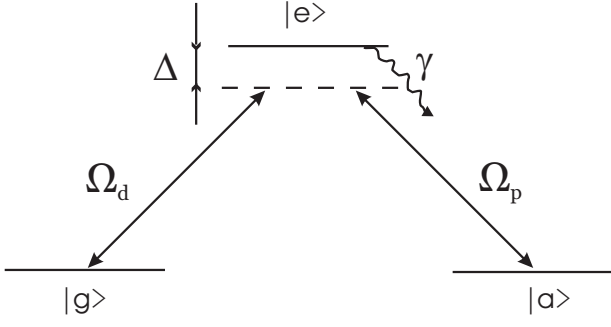


FIG. 1. Three-level system coupled by two lasers. Ω_p and Ω_d are the Rabi frequencies for the pump and dump laser, Δ is the one photon detuning, and γ is the loss rate.

as ψ_e , ψ_a , and ψ_g respectively, we get the Schroedinger equation:

$$i\dot{\psi}_a = \Omega_p \psi_e, \quad (2a)$$

$$i\dot{\psi}_e = -(\Delta + i\gamma)\psi_e + \Omega_p \psi_a + \Omega_d \psi_g, \quad (2b)$$

$$i\dot{\psi}_g = \Omega_d \psi_e. \quad (2c)$$

The normalization reads:

$$|\psi_a(t)|^2 + |\psi_g(t)|^2 + |\psi_e(t)|^2 \leq 1, \quad (3)$$

where equality holds for initial time. Because of losses ($\gamma > 0$) the total normalization will be slightly reduced (for $t > 0$) during the transfer of population through the excited level.

We take the laser pulses to be Gaussian

$$\Omega_d = \Omega_0 \exp[-(t - t_d)^2], \quad (4a)$$

$$\Omega_p = \Omega_0 \exp[-(t - t_p)^2]. \quad (4b)$$

The third order system (2) may be rewritten in a matrix form

$$\dot{\Psi} = -iH\Psi \equiv A\Psi, \quad (5)$$

where $\Psi = [\psi_a, \psi_e, \psi_g]^T$ is the vector of the state of the system, and

$$H = \begin{pmatrix} 0 & \Omega_p & 0 \\ \Omega_p & -(\Delta + i\gamma) & \Omega_d \\ 0 & \Omega_d & 0 \end{pmatrix} \quad (6)$$

is the corresponding Hamiltonian. The matrix $A \equiv -iH$ is the Jacobian of the system. If the Hamiltonian possesses eigenvalues ω , then the eigenvalues of the Jacobian are defined by $\lambda = -i\omega$. Note that the real parts of λ determine the stability of the fixed point at the origin.

We now find these eigenvalues, more specifically their real parts. The eigenvalues of Hamiltonian satisfy the characteristic equation

$$\det[H - I\omega] = 0. \quad (7)$$

Expanding the corresponding third-order determinant one finds that one eigenvalue is always zero:

$$\omega_1 = 0. \quad (8)$$

The other two eigenvalues satisfy the quadratic equation:

$$\omega^2 + (\Delta + i\gamma)\omega - (\Omega_d^2 + \Omega_p^2) = 0. \quad (9)$$

Thus the two eigenvalues satisfy

$$\omega_2 + \omega_3 = -[\Delta + i\gamma], \quad (10a)$$

$$\omega_2 \omega_3 = -[\Omega_d^2 + \Omega_p^2]. \quad (10b)$$

Assuming $\Delta = 0$, the solutions of (9) read:

$$\omega_{2,3} = (-i\gamma \pm [-\gamma^2 + 4(\Omega_d^2 + \Omega_p^2)]^{1/2})/2. \quad (11)$$

For $t \rightarrow \pm\infty$ the Rabi frequencies go to zero, and it follows from Eq. (10) that $\omega_2 = 0, \omega_3 = -i\gamma$. Calling on Eq. (8), we can write

$$\lambda_{1,2} = 0, \quad \lambda_3 = -\gamma, \quad (12)$$

or $\text{Re}(\lambda_{1,2}) = 0$, and $\text{Re}(\lambda_3) = -\gamma$ for $t \rightarrow \pm\infty$.

For finite times there is a region where the Rabi frequencies are large enough, so that the discriminant is positive in Eq. (11): $D \equiv -\gamma^2 + 4(\Omega_d^2 + \Omega_p^2) > 0$. Such a situation occurs in a certain interval $t_1 < t < t_2$, and from (11) we get

$$\omega_{2,3} = -i\gamma/2 \pm \sqrt{D}/2, \quad (13a)$$

$$\lambda_{2,3} = -\gamma/2 \mp i\sqrt{D}/2. \quad (13b)$$

The first eigenvalue is $\lambda_1 = \omega_1 = 0$. The boundaries t_1, t_2 are solutions of $D(t) = 0$ in respect to time.

Hence, in the interval $t_1 < t < t_2$, the real parts are $\text{Re}(\lambda_1) = 0, \text{Re}(\lambda_{2,3}) = -\gamma/2$.

We may adiabatically reduce the dimension of this system but we first transform its variables. We change the bare variables ψ_a, ψ_g to the bright ψ_B and dark ψ_D one:

$$\psi_B = (\Omega_p \psi_a + \Omega_d \psi_g)/\Omega, \quad (14a)$$

$$\psi_D = (\Omega_d \psi_a - \Omega_p \psi_g)/\Omega, \quad (14b)$$

where

$$\Omega = [\Omega_p^2 + \Omega_d^2]^{1/2}. \quad (15)$$

Denoting $\xi_p = \Omega_p/\Omega, \xi_d = \Omega_d/\Omega$, and performing some operations, we obtain the following equations for the new variables:

$$i\dot{\psi}_B = \alpha \psi_D + \Omega \psi_e, \quad (16a)$$

$$i\dot{\psi}_e = -(\Delta + i\gamma)\psi_e + \Omega \psi_B, \quad (16b)$$

$$i\dot{\psi}_D = \alpha^* \psi_B, \quad (16c)$$

with $\alpha = i(\dot{\xi}_p \xi_d - \dot{\xi}_d \xi_p)$.

We now apply the adiabatic approximation to this system by setting $\dot{\psi}_e = 0$. From Eq.(16b) we get

$$\psi_e = \frac{\Omega}{\Delta + i\gamma} \psi_B. \quad (17)$$

Inserting this result in (16) we obtain

$$i\dot{\psi}_B = \alpha\psi_D + \frac{\Omega^2}{\Delta + i\gamma}\psi_B, \quad (18a)$$

$$i\dot{\psi}_D = \alpha^*\psi_B. \quad (18b)$$

We solve this system to find the dynamics of ψ_B , ψ_D , and from (17) we find the dynamics of ψ_e .

The system (18) may be also adiabatically reduced. We now set $\dot{\psi}_B = 0$, and solve the Eq.(18a) for ψ_B :

$$\psi_B = -\frac{\alpha(\Delta + i\gamma)}{\Omega^2}\psi_D. \quad (19)$$

Inserting this result in Eq.(18b), we get a first order dynamic system

$$i\dot{\psi}_D = -\frac{|\alpha|^2(\Delta + i\gamma)}{\Omega^2}\psi_D. \quad (20)$$

We now may determine the ranges where the obtained equations are valid. First of all, the exact 3D equations (2) and (16) are valid for all times t . Next, we note that for $t \rightarrow \pm\infty$, the process is 2D since in these ranges two real parts $\text{Re}(\lambda_{1,2}) = 0$ are zeros, and the third real part is a negative number, $\text{Re}(\lambda_3) = -\gamma$. Therefore one may use Eq.(18) in this range. Lastly, for $t_1 < t < t_2$, the dynamics is 1D, since only one real part $\text{Re}(\lambda_1) = 0$ is zero, and the rest two real parts are negative, $\text{Re}(\lambda_{2,3}) = -\gamma/2$. We thus conclude that in the range $t_1 < t < t_2$ Eq.(20) is valid.

Note that we determined the range of validity for Eq.(18) as plus-minus infinity. However, the Rabi frequencies $\Omega_p(t)$ and $\Omega_d(t)$ are chosen in the form of Gaussian pulses that remain close to zero for an extended interval of time, and they grow up (decay) very rapidly. Therefore in (10b) one may suppose that $[\Omega_d^2 + \Omega_p^2] \simeq 0$ for $t < t_1$ and $t > t_2$. We then may approximately set $\text{Re}(\lambda_2) \simeq 0$, and $\text{Re}(\lambda_3) \simeq -\gamma$ in this range.

Summing up, the Eqs.(16), (2), and (18) are valid everywhere, whereas the Eq.(20) is valid for $t_1 < t < t_2$. The dynamics of $\text{Re}(\lambda(t))$ is shown in Fig.2.

III. THE LINEAR TRIPOD

The STIRAP process in the linear tripod scheme without dissipation was first considered by Unanyan *et al.* [13, 14]. Here we outline this scheme in which the dissipation is also included. Afterwards we perform the linear analysis of this system.

Consider the four-level system schematically shown in Fig.3. The excited state $|e\rangle$ is coupled to three ground

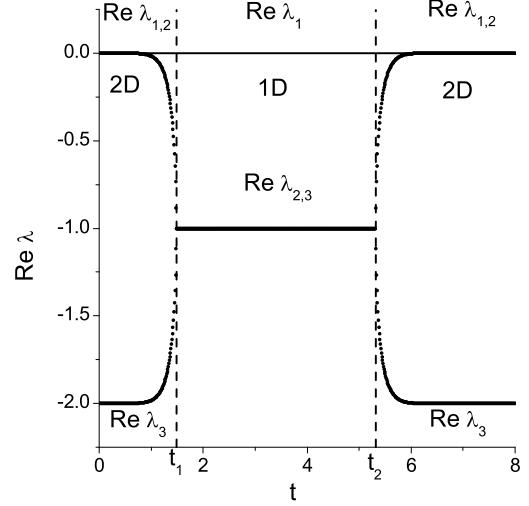


FIG. 2. Dynamics of real parts of eigenvalues of the Jacobian for linear lambda system, computed by (11), and (8). The dashed vertical lines set the boundaries for the 1D and 2D processes. Here $t_1 = 1.49$ and $t_2 = 5.32$. The parameters are as follows: $\Delta = 0$, $\gamma = 2.0$, $\Omega_0 = 10.0$, $t_p = 3.8$, $t_d = 3.0$.

states $|a\rangle$, $|g_1\rangle$, and $|g_2\rangle$ with the coupling strengths denoted as Ω_p , Ω_{d1} , and Ω_{d2} , respectively. Here p stands for pump and d stands for the damp. The four-level Hamiltonian reads:

$$H = -\hbar(\Delta + i\gamma)|e\rangle\langle e| + \frac{\hbar}{2}[\Omega_p|a\rangle\langle e| + \Omega_{d1}|g_1\rangle\langle e| + \Omega_{d2}|g_2\rangle\langle e| + H.c.]. \quad (21)$$

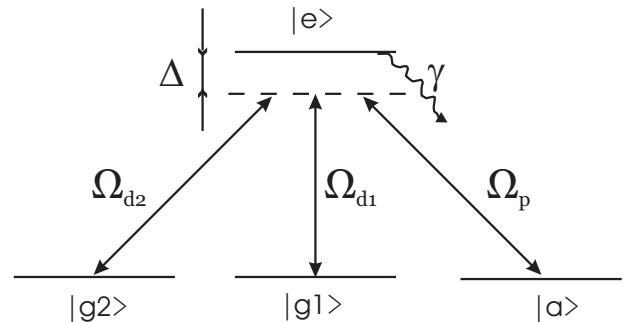


FIG. 3. Four-level system coupled by three lasers. Ω_p and Ω_{d1} , Ω_{d2} are the Rabi frequencies for the pump, and damp lasers, Δ is the one photon detuning, and γ is the loss rate.

Denoting the amplitudes as ψ_e , ψ_a , ψ_{g1} , and ψ_{g2} , the

Schroedinger equation reads:

$$i\dot{\psi}_a = \Omega_p \psi_e, \quad (22a)$$

$$i\dot{\psi}_e = -(\Delta + i\gamma)\psi_e + \Omega_p \psi_a + \Omega_{d1}\psi_{g1} + \Omega_{d2}\psi_{g2}, \quad (22b)$$

$$i\dot{\psi}_{g1} = \Omega_{d1}\psi_e, \quad (22c)$$

$$i\dot{\psi}_{g2} = \Omega_{d2}\psi_e. \quad (22d)$$

The normalization is given by

$$|\psi_a(t)|^2 + |\psi_{g1}(t)|^2 + |\psi_{g2}(t)|^2 + |\psi_e(t)|^2 \leq 1, \quad (23)$$

where equality holds for initial time. Because of losses ($\gamma > 0$) the total normalization will be slightly reduced (for $t > 0$) during the transfer of population through the excited state.

The Rabi frequencies are given by

$$\Omega_p = \Omega_0 \exp[-(t - t_p)^2], \quad (24a)$$

$$\Omega_{d1} = K_1 \Omega_0 \exp[-(t - t_{d1})^2], \quad (24b)$$

$$\Omega_{d2} = K_2 \Omega_0 \exp[-(t - t_{d2})^2]. \quad (24c)$$

The system (22) can be written in the form of Eq.(5) with the state vector $\Psi = [\psi_a, \psi_e, \psi_{g1}, \psi_{g2}]^T$, and Hamiltonian

$$H = \begin{pmatrix} 0 & \Omega_p & 0 & 0 \\ \Omega_p & -(\Delta + i\gamma) & \Omega_{d1} & \Omega_{d2} \\ 0 & \Omega_{d1} & 0 & 0 \\ 0 & \Omega_{d2} & 0 & 0 \end{pmatrix}. \quad (25)$$

The matrix A is again the Jacobian of the system. Because of $A = -iH$, the relation $\lambda = -i\omega$ holds. Solving the eigenvalues problem (7) for the linear tripod, we obtain two zero eigenvalues,

$$\omega_{1,2} = 0. \quad (26)$$

The other two eigenvalues can be found from quadratic equation

$$\omega^2 + (\Delta + i\gamma)\omega - (\Omega_{d1}^2 + \Omega_{d2}^2 + \Omega_p^2) = 0. \quad (27)$$

The eigenvalues $\omega_{3,4}$ must satisfy

$$\omega_3 + \omega_4 = -[\Delta + i\gamma], \quad (28a)$$

$$\omega_3 \omega_4 = -[\Omega_{d1}^2 + \Omega_{d2}^2 + \Omega_p^2]. \quad (28b)$$

We again assume that $\Delta = 0$, thus obtaining the following solutions:

$$\omega_{3,4} = (-i\gamma \pm [-\gamma^2 + 4(\Omega_{d1}^2 + \Omega_{d2}^2 + \Omega_p^2)]^{1/2})/2. \quad (29)$$

(See also Eq.(7) in [14]). The Rabi frequencies are chosen in the form of Gaussian pulses. For $t \rightarrow \pm\infty$ the Rabi frequencies tend to zero, and from (28) it follows that $\omega_3 = 0$, $\omega_4 = -i\gamma$. Hence, for $t \rightarrow \pm\infty$ we have

$$\lambda_{1,2,3} = 0, \quad \lambda_4 = -\gamma. \quad (30)$$

However between these two infinite times there is a region where the Rabi frequencies are large enough, and the discriminant in (29) is positive ($D \equiv -\gamma^2 + 4(\Omega_{d1}^2 + \Omega_{d2}^2 + \Omega_p^2) > 0$). Such a situation takes place in the interval $t_1 < t < t_2$, and from (29) we get

$$\omega_{3,4} = -i\gamma/2 \pm \sqrt{D}/2, \quad (31a)$$

$$\lambda_{3,4} = -\gamma/2 \mp i\sqrt{D}/2. \quad (31b)$$

The first two eigenvalues are $\lambda_{1,2} = \omega_{1,2} = 0$. The boundaries t_1, t_2 are solutions of $D(t) = 0$ in respect to time.

Hence, in the interval $t_1 < t < t_2$, the real parts are $\text{Re}(\lambda_{1,2}) = 0$, $\text{Re}(\lambda_{3,4}) = -\gamma/2$.

Exactly as in the previous section, we first transform the variables from the bare states to one bright and two dark states:

$$(\psi_a, \psi_e, \psi_{g1}, \psi_{g2}) \rightarrow (\psi_B, \psi_e, \psi_{D1}, \psi_{D2}). \quad (32)$$

Parameterizing the Rabi frequencies as

$$\Omega_{d2} = \Omega \sin(\phi), \quad (33a)$$

$$\Omega_p = \Omega \cos(\phi) \sin(\Theta), \quad (33b)$$

$$\Omega_{d1} = \Omega \cos(\phi) \cos(\Theta), \quad (33c)$$

we may write down the amplitudes of one bright and two dark states:

$$\psi_B = \cos(\phi) \sin(\Theta) \psi_a + \cos(\phi) \cos(\Theta) \psi_{g1} + \sin(\phi) \psi_{g2}, \quad (34a)$$

$$\psi_{D1} = \cos(\Theta) \psi_a - \sin(\Theta) \psi_{g1}, \quad (34b)$$

$$\psi_{D2} = \sin(\phi) \sin(\Theta) \psi_a + \sin(\phi) \cos(\Theta) \psi_{g1} - \cos(\phi) \psi_{g2}. \quad (34c)$$

After some operations, we derive the following dynamic system for these variables:

$$i \frac{d}{dt} \begin{pmatrix} \psi_B \\ \psi_e \\ \psi_{D1} \\ \psi_{D2} \end{pmatrix} = \begin{pmatrix} 0 & \Omega & \alpha_{13} & \alpha_{14} \\ \Omega & -(\Delta + i\gamma) & 0 & 0 \\ \alpha_{13}^* & 0 & 0 & \alpha_{34} \\ \alpha_{14}^* & 0 & \alpha_{34}^* & 0 \end{pmatrix} \begin{pmatrix} \psi_B \\ \psi_e \\ \psi_{D1} \\ \psi_{D2} \end{pmatrix}. \quad (35)$$

Here

$$\alpha_{13} = i(\dot{\xi}_{11}\xi_{31} + \dot{\xi}_{13}\xi_{33}), \quad (36a)$$

$$\alpha_{14} = i(\dot{\xi}_{11}\xi_{41} + \dot{\xi}_{13}\xi_{43} + \dot{\xi}_{14}\xi_{44}), \quad (36b)$$

$$\alpha_{34} = i(\dot{\xi}_{31}\xi_{41} + \dot{\xi}_{33}\xi_{43}), \quad (36c)$$

and the coefficients ξ_{ij} are defined by the matrix

$$\|\xi_{ij}\| = \begin{pmatrix} \cos(\phi) \sin(\Theta) & 0 & \cos(\phi) \cos(\Theta) & \sin(\phi) \\ 0 & 1 & 0 & 0 \\ \cos(\Theta) & 0 & -\sin(\Theta) & 0 \\ \sin(\phi) \sin(\Theta) & 0 & \sin(\phi) \cos(\Theta) & -\cos(\phi) \end{pmatrix}. \quad (37)$$

Note that this matrix realizes the transformation (32) (see also Eqs.(34)).

We now reduce the dimension of system (35) in two steps. For the first step, we eliminate the excited state by setting

$$\dot{\psi}_e = 0. \quad (38)$$

Solving the equation

$$\Omega\psi_B - (\Delta + i\gamma)\psi_e = 0, \quad (39)$$

(see the second row in (35)) for ψ_e , we get

$$\psi_e = \frac{\Omega}{\Delta + i\gamma}\psi_B. \quad (40)$$

Inserting this result in (35), we obtain the following three-dimensional dynamic system:

$$i\frac{d}{dt}\begin{pmatrix} \psi_B \\ \psi_{D1} \\ \psi_{D2} \end{pmatrix} = \begin{pmatrix} \frac{\Omega^2}{\Delta + i\gamma} & \alpha_{13} & \alpha_{14} \\ \alpha_{13}^* & 0 & \alpha_{34} \\ \alpha_{14}^* & \alpha_{34}^* & 0 \end{pmatrix} \begin{pmatrix} \psi_B \\ \psi_{D1} \\ \psi_{D2} \end{pmatrix}. \quad (41)$$

We can solve this system to find the evolution of ψ_B , ψ_{D1} , ψ_{D2} , and to determine the dynamics of the excited state using (40).

For the second step, we eliminate the bright state, i.e. we set

$$\dot{\psi}_B = 0, \quad (42)$$

in Eqs.(41). After solving the equation

$$\frac{\Omega^2}{\Delta + i\gamma}\psi_B + \alpha_{13}\psi_{D1} + \alpha_{14}\psi_{D2} = 0 \quad (43)$$

for ψ_B (see the first row in (41)), we find

$$\psi_B = -\frac{\Delta + i\gamma}{\Omega^2}(\alpha_{13}\psi_{D1} + \alpha_{14}\psi_{D2}). \quad (44)$$

Inserting this result in Eq.(41), we obtain the following second order system:

$$i\frac{d}{dt}\begin{pmatrix} \psi_{D1} \\ \psi_{D2} \end{pmatrix} = A \begin{pmatrix} \psi_{D1} \\ \psi_{D2} \end{pmatrix}. \quad (45)$$

The matrix of this system may be split into two parts:

$$A = A_0 + \frac{\Delta + i\gamma}{\Omega^2}A_1, \quad (46)$$

where

$$A_0 = \begin{pmatrix} 0 & \alpha_{34} \\ \alpha_{34}^* & 0 \end{pmatrix}, \quad (47)$$

and

$$A_1 = -\begin{pmatrix} |\alpha_{13}|^2 & \alpha_{13}^*\alpha_{14} \\ \alpha_{14}^*\alpha_{13} & |\alpha_{14}|^2 \end{pmatrix}. \quad (48)$$

When Ω^2 is relatively large, one can neglect the influence of A_1 and write approximately $A \simeq A_0$. Thus one arrives at a simple second order system

$$i\frac{d}{dt}\begin{pmatrix} \psi_{D1} \\ \psi_{D2} \end{pmatrix} = \begin{pmatrix} 0 & \alpha_{34} \\ \alpha_{34}^* & 0 \end{pmatrix} \begin{pmatrix} \psi_{D1} \\ \psi_{D2} \end{pmatrix}. \quad (49)$$

which is equivalent to Eq.(27) of ref. [13]. We now discuss the validity of 4D, 3D and 2D equations. The 4D Eqs.(22) and (35) are valid everywhere. Next, in the ranges $t < t_1$ and $t > t_2$ the process is 3D since there are three zero real parts, $\text{Re}(\lambda_{1,2,3}) \simeq 0$, and one negative real part, $\text{Re}(\lambda_4) \simeq -\gamma$. Therefore Eq.(41) is valid in this interval. In the region where $t_1 < t < t_2$, the process is 2D since there are two zero real parts, $\text{Re}(\lambda_{1,2}) = 0$ and two negative real parts, $\text{Re}(\lambda_{3,4}) = -\gamma/2$. Here Eq.(49) holds.

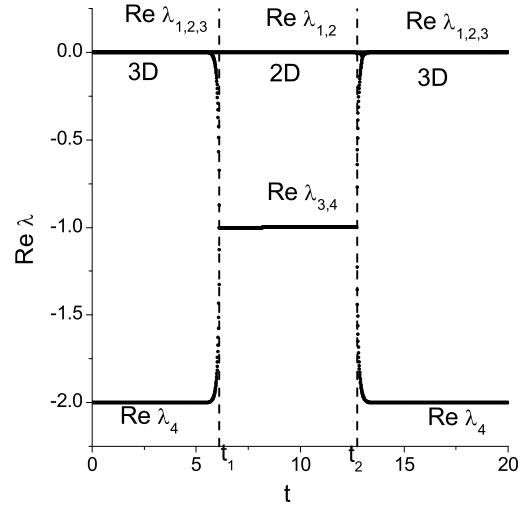


FIG. 4. Dynamics of real parts of eigenvalues of the Jacobian for linear tripod, computed by (29), and (26). The dashed vertical lines set the boundaries for the 2D and 3D processes. Here $t_1 = 6.12$ and $t_2 = 12.73$. The parameters are as follows: $\Delta = 0$, $\gamma = 2.0$, $\Omega_0 = 60.0$, $t_p = 10.7$, $t_{d1} = 10.0$, $t_{d2} = 8.5$, $K_1 = 0.75$, $K_2 = 5.0$.

Summing up, the Eqs.(22), (35), and (41) are valid everywhere, whereas the Eq.(49) is valid in the range $t_1 < t < t_2$. In Fig.4 the dynamics of $\text{Re}(\lambda(t))$ is presented. Fig.5 displays the results of numerical computations. In Fig.5(a) we have presented the dynamics of populations of the bright (solid black and red lines), and excited (dashed black and red lines) states. The black lines correspond to solutions of exact equation (22). The red lines are obtained from Eq.(41) (the bright state), and from Eq.(40) (the excited state). One can see that the populations of these states remain relatively small ($P_e, P_B \simeq 10^{-3}$). In Fig.5(b) the dynamics of coupling strengths is shown. Figures 5(c,d) display the dynamics of populations of the degenerate dark states. Figure

5(c) presents the solutions of exact Eqs.(22) (black line) and that of adiabatically reduced system (41) (red line). The exact and approximate solutions are in good quantitative agreement. Both systems were integrated in the whole time range ($t \in [0.0, 20.0]$). In Fig.5(d) we compare the dynamics for exact Eqs.(22) (black line) with those of adiabatically simplified Eqs.(49). The latter system was integrated in the time range $t \in [3.0, 13.0]$ in which the quantity $\Omega^2(t)$ is relatively large.

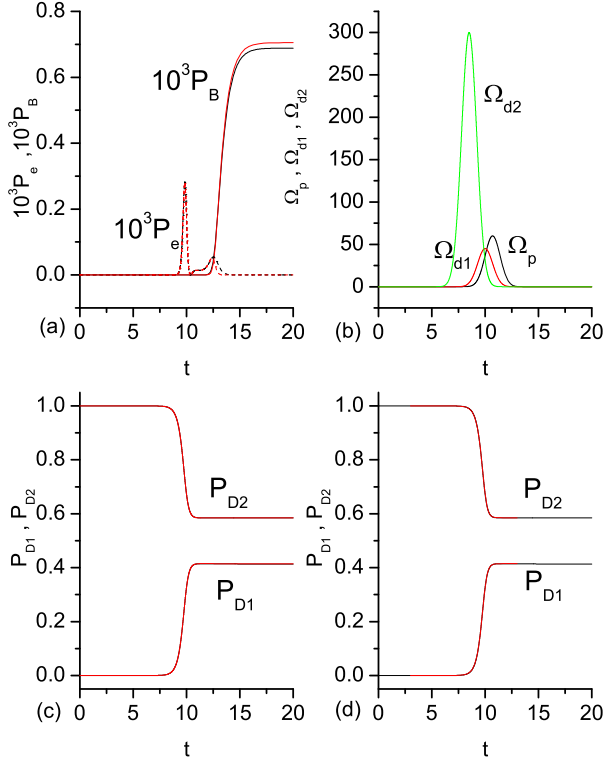


FIG. 5. (Color online) (a) The dynamics of populations $10^3 P_e, 10^3 P_B$ that are computed from (22) (black lines), and from (41), (40) (red lines); (b) the dynamics of Gaussian pulses computed by (24); (c,d) the dynamics of populations of dark states computed in (c) by (22) (black), and by (41) (red); in (d) the black line represents again the exact solution of (22), and red line is obtained using the adiabatic approximation from Eqs.(49) (integrated in the range $t \in [3.0, 13.0]$). The parameters are the same as in Fig.4. The initial conditions are $\psi_a(0) = 1$, $\psi_{g1}(0) = \psi_{g2}(0) = \psi_e(0) = 0$.

IV. THE NONLINEAR LAMBDA SYSTEM

The three-level nonlinear Hamiltonian for the nonlinear lambda system (see the Fig.1) reads:

$$H = -\hbar(\Delta + i\gamma)\psi_e^\dagger\psi_e + \frac{\hbar}{2}(\Omega_p\psi_e^\dagger\psi_a\psi_a + \Omega_d\psi_e^\dagger\psi_g + H.c.). \quad (50)$$

The Heisenberg equation leads to the following equations of motion for the amplitudes of the nonlinear lambda system:

$$i\dot{\psi}_a = \Omega_p\psi_a^*\psi_e, \quad (51a)$$

$$i\dot{\psi}_e = -(\Delta + i\gamma)\psi_e + \frac{1}{2}\Omega_p\psi_a^2 + \frac{1}{2}\Omega_d\psi_g, \quad (51b)$$

$$i\dot{\psi}_g = \frac{1}{2}\Omega_d\psi_e. \quad (51c)$$

The normalization reads:

$$|\psi_a(t)|^2 + 2[|\psi_g(t)|^2 + |\psi_e(t)|^2] \leq 1, \quad (52)$$

where the equality holds for the initial time. Because of losses ($\gamma > 0$) the total normalization will be slightly reduced (for $t > 0$) during the transfer of population through the excited level.

As for the linear lambda system, we take the Gaussian pulses given by Eqs.(4).

Similarly as in two previous sections, we here define the state vector $\Psi = [\psi_a, \psi_e, \psi_g]^T$. The dynamic system (51) can be rewritten in the vector form:

$$i\frac{d}{dt}\Psi = \mathbf{f}(\Psi), \quad (53)$$

where \mathbf{f} is the vector of (generally) nonlinear functions on the r.h.s. of system (51). The steady state solution $\Psi_0(t)$ of this system represents the dark state which is obtained by solving

$$\mathbf{f}(\Psi_0) = 0. \quad (54)$$

For the nonlinear lambda system (51) the dark state reads ([29, 47]):

$$\psi_a^0 = \left[\frac{2\Omega_d}{\Omega_d + \Omega_{eff}} \right]^{1/2}, \quad \psi_e^0 = 0, \quad \psi_g^0 = -\frac{2\Omega_p}{\Omega_d + \Omega_{eff}}, \quad (55)$$

with $\Omega_{eff} = [\Omega_d^2 + 8\Omega_p^2]^{1/2}$.

If the solution remains in this state for the whole time, the adiabatic passage from initially occupied state a to the target state g takes place provided the Gaussian pulses $\Omega_d(t)$, $\Omega_p(t)$ arrive in a counter-intuitive sequence.

We are now interested in the linear stability of the dark state (55). To this end, we suppose that the solution of Eq. (53) evolves in the close neighborhood of the dark state Ψ_0 , i.e. we express it as a sum

$$\Psi(t) = \Psi_0(t) + \delta\Psi(t), \quad (56)$$

where $\delta\Psi(t)$ is a deviation of the current solution from the dark state. Inserting this expression in (53) yields

$$i\dot{\Psi}_0(t) + i\frac{d}{dt}\delta\Psi(t) = \mathbf{f}(\Psi_0(t) + \delta\Psi(t)). \quad (57)$$

Using the Eq.(54), one finds

$$i\frac{d}{dt}\delta\Psi = M\delta\Psi - i\dot{\Psi}_0. \quad (58)$$

where M is a matrix with the elements $M_{ij} = \frac{\partial f_i}{\partial \psi_j}$ with $i, j = a, e, g$. Here the partial derivatives are calculated at the dark state. In system of equations (58) the nonlinear terms have been omitted.

Specifically, for the system of equations (51), the matrix M reads

$$M = \begin{pmatrix} 0 & \Omega_p \psi_a^{0*} & 0 \\ \Omega_p \psi_a^0 & -(\Delta + i\gamma) & \Omega_d/2 \\ 0 & \Omega_d/2 & 0 \end{pmatrix}. \quad (59)$$

(See also Eq.(7) in [23]). It is similar to the Hamiltonian (6) of the linear lambda system. The difference is that the elements M_{ae} and M_{ea} contain the component of the dark state ψ_a^0 due to the nonlinearity.

Denoting the Jacobian as $A = -iM$, we can rewrite the linearized equation (58) as

$$\frac{d}{dt} \delta \Psi = A \delta \Psi - \dot{\Psi}_0. \quad (60)$$

In this system, the real parts of the eigenvalues of the Jacobian A determine the stability of the dark state. If the matrix M has eigenvalues ω , the Jacobian A has the eigenvalues $\lambda = -i\omega$. In analogy to the linear lambda system, the eigenvalues ω can be found from the characteristic equation

$$\det ||M - I\omega|| = 0. \quad (61)$$

Solving Eqs.(61) with (59), we find that one root is always zero:

$$\omega_1 = 0. \quad (62)$$

The other two eigenvalues obey the quadratic equation:

$$\omega^2 + (\Delta + i\gamma)\omega - (\Omega_d^2 + 4\Omega_p^2|\psi_a^0|^2)/4 = 0. \quad (63)$$

The corresponding eigenvalues ω_2 and ω_3 obey the following

$$\omega_2 + \omega_3 = -[\Delta + i\gamma], \quad (64a)$$

$$\omega_2 \omega_3 = -[\Omega_d^2 + 4\Omega_p^2|\psi_a^0|^2]/4. \quad (64b)$$

By setting $\Delta = 0$, we get the solutions of quadratic equation:

$$\omega_{2,3} = (-i\gamma \pm [-\gamma^2 + \Omega_d^2 + 4\Omega_p^2|\psi_a^0|^2]^{1/2})/2. \quad (65)$$

(See also the equations under Eq.(7) in [23]). For $t \rightarrow \pm\infty$, it follows from (64) that $\omega_2 = 0$ and $\omega_3 = -i\gamma$. The corresponding eigenvalues of Jacobian read:

$$\lambda_{1,2} = 0, \quad \lambda_3 = -\gamma, \quad (66)$$

or $\text{Re}(\lambda_{1,2}) = 0$, and $\text{Re}(\lambda_3) = -\gamma$ for $t \rightarrow \pm\infty$.

Between these two infinities there is a region where the discriminant is positive, $D \equiv -\gamma^2 + \Omega_d^2 + 4\Omega_p^2|\psi_a^0|^2 > 0$. The latter condition is satisfied in the range $t_1 < t < t_2$,

where $t_{1,2}$ are the solutions of $D(t) = 0$. In this region one has

$$\omega_{2,3} = -i\gamma/2 \pm \sqrt{D}/2, \quad (67a)$$

$$\lambda_{2,3} = -\gamma/2 \mp i\sqrt{D}/2. \quad (67b)$$

We have in this range $\text{Re}(\lambda_1) = 0$ and $\text{Re}(\lambda_{2,3}) = -\gamma/2$.

We note that the Rabi frequencies $\Omega_p(t)$ and $\Omega_d(t)$ are chosen in the form of Gaussian pulses that remain close to zero for a long space of time, and they grow up (decay) very rapidly. Therefore in (64b) one may suppose that $[\Omega_d^2 + 4\Omega_p^2|\psi_a^0|^2]/4 \simeq 0$ for $t < t_1$ and $t > t_2$. We then may approximately evaluate $\text{Re}(\lambda_2) \simeq 0$ and $\text{Re}(\lambda_3) \simeq -\gamma$ in this range.

We now adiabatically eliminate the excited state by setting $\psi_e = 0$. From Eq.(51b) we get

$$\psi_e = \frac{1}{2(\Delta + i\gamma)}(\Omega_p \psi_a^2 + \Omega_d \psi_g). \quad (68)$$

Inserting this result into Eq.(51) we obtain a second order system

$$i\dot{\psi}_a = \Omega_p \psi_a^* \psi_e, \quad (69a)$$

$$i\dot{\psi}_g = \frac{1}{2}\Omega_d \psi_e. \quad (69b)$$

with ψ_e given by Eq.(68).

We now discuss the validity of 3D and 2D systems. The 3D system (51) is valid for all times. In the ranges $t < t_1$ and $t > t_1$ the 2D system (69) can be applied since there are two zero real parts $\text{Re}(\lambda_{1,2}) = 0$, and one negative real part $\text{Re}(\lambda_3) = -\gamma$. In the range $t_1 < t < t_2$ the process is 1D since there is only one zero real part $\text{Re}(\lambda_1) = 0$ and two negative real parts $\text{Re}(\lambda_{2,3}) = -\gamma/2$. However, here we do not have any 1D equation, one can only propose the 2D system (69). The search for a 1D system is a challenging problem. In Fig.6 we show the dynamics of $\text{Re}(\lambda(t))$.

In the Fig.7 we have plotted the relevant dynamics for the case of adiabatically approximated nonlinear lambda system. In the Fig.7(a) we show the Gaussian pulses that are ordered counter-intuitively. From Fig.7(b) one may conclude that the solutions of adiabatically approximated system are in good quantitative agreement with the solutions of exact system. In Fig.7(c) we see that the difference for P_e between exact and approximated solutions is significant. It can be explained by the fact that the magnitude of probability P_e is small. On the other hand, the difference in the case of P_a , P_g is of the same order but we do not distinguish it, since the magnitudes of these quantities are much larger. In Fig.7(d) we have plotted the dynamics of the difference between the exact (P_a) and adiabatically approximate (P_a^{ad}) solutions of the population P_a . (See also the blue line in Fig.2(c) in [25]). The difference is of the same order as that in Fig.7(c).

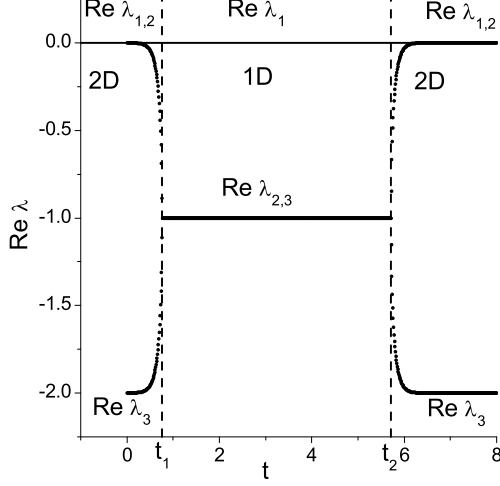


FIG. 6. Dynamics of real parts of eigenvalues of the Jacobian for nonlinear lambda system, computed by (65), and (62). The dashed vertical lines set the boundaries for the 1D and 2D processes. Here $t_1 = 0.76$ and $t_2 = 5.71$. The parameters are as follows: $\Delta = 0$, $\gamma = 2.0$, $\Omega_0 = 300.0$, $t_p = 3.8$, $t_d = 3.0$.

V. THE NONLINEAR TRIPOD

The four-level nonlinear Hamiltonian for nonlinear tripod depicted in Fig.3 reads:

$$H = -\hbar(\Delta + i\gamma)\psi_e^\dagger\psi_e + \frac{\hbar}{2}(\Omega_p\psi_e^\dagger\psi_a\psi_a + \Omega_{d1}\psi_e^\dagger\psi_{g1} + \Omega_{d2}\psi_e^\dagger\psi_{g2} + H.c.). \quad (70)$$

The Heisenberg equation leads to the following equations of motion for the amplitudes of the nonlinear tripod:

$$i\dot{\psi}_a = \Omega_p\psi_a^*\psi_e, \quad (71a)$$

$$i\dot{\psi}_e = -(\Delta + i\gamma)\psi_e + \frac{1}{2}\Omega_p\psi_a^2 + \frac{1}{2}\Omega_{d1}\psi_{g1} + \frac{1}{2}\Omega_{d2}\psi_{g2}, \quad (71b)$$

$$i\dot{\psi}_{g1} = \frac{1}{2}\Omega_{d1}\psi_e, \quad (71c)$$

$$i\dot{\psi}_{g2} = \frac{1}{2}\Omega_{d2}\psi_e. \quad (71d)$$

The normalization reads:

$$|\psi_a(t)|^2 + 2[|\psi_{g1}(t)|^2 + |\psi_{g2}(t)|^2 + |\psi_e(t)|^2] \leq 1, \quad (72)$$

where the equality holds for the initial time. Because of losses ($\gamma > 0$) the normalization will be slightly reduced (for $t > 0$) during the adiabatic transfer of population through the excited state.

Like in the case of linear tripod, the Gaussian pulses are given by Eqs.(24).

Similar to the linear case, we define the following state vector of the system: $\Psi = [\psi_a, \psi_e, \psi_{g1}, \psi_{g2}]^T$. The dynamic equations (71) can be rewritten in a vector form given by Eq. (53), where \mathbf{f} is now the vector of nonlinear functions on the r.h.s of Eq.(71). The manifold of the steady states of this system represents the dark state $\Psi_0 = [\psi_a^0, \psi_e^0, \psi_{g1}^0, \psi_{g2}^0]^T$. This manifold has to satisfy the Eq.(54) and the condition of normalization. Since $\psi_e^0 = 0$, the dark state obeys the following:

$$\Omega_p(\psi_a^0)^2 + \Omega_{d1}\psi_{g1}^0 + \Omega_{d2}\psi_{g2}^0 = 0, \quad (73a)$$

$$|\psi_a^0|^2 + 2|\psi_{g1}^0|^2 + 2|\psi_{g2}^0|^2 = 1, \quad (73b)$$

$$\psi_e^0 = 0. \quad (73c)$$

We are interested in the linear stability of this dark state. Therefore we suppose that the solution of Eq.(71) evolves in the close neighborhood of the dark state Ψ_0 , i.e. we express it as a sum given by Eq.(56) where $\delta\Psi(t)$ is the deviation of the current solution from the dark state.

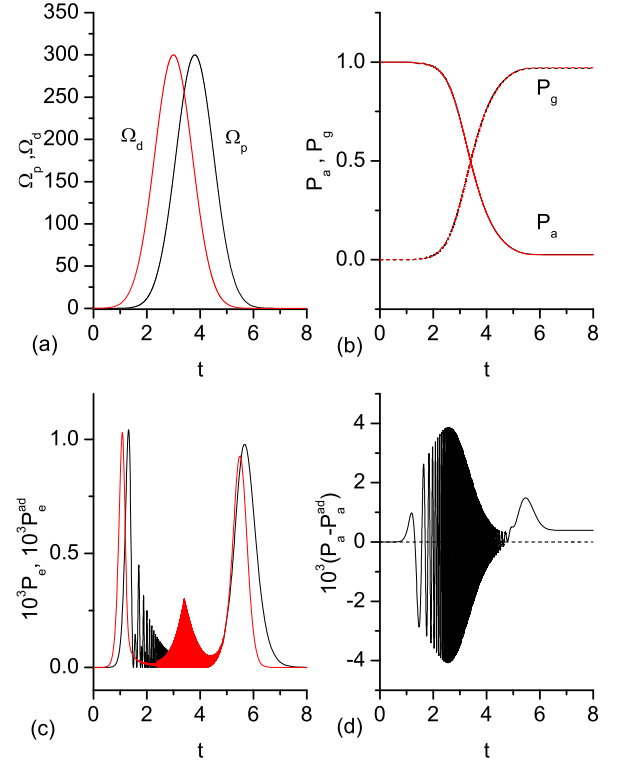


FIG. 7. (Color online) The dynamics (a) of Gaussian pulses (4), (b) of populations P_a , P_g , (c) of population P_e in enlarged scale, and (d) the difference of P_a between exactly (P_a) and adiabatically (P_a^{ad}) obtained solutions. In (b,c) the black lines represent the solutions of exact Eqs.(51), and the red lines are the solutions of adiabatically approximated system (69) with excited state given by (68). The parameters are the same as in Fig.6. The initial conditions are $\psi_a(0) = 1$, $\psi_g(0) = \psi_e(0) = 0$.

Hence one arrives at a linearized equation similar to the one for the nonlinear lambda system

$$i \frac{d}{dt} \delta \Psi = M \delta \Psi - i \dot{\Psi}_0. \quad (74)$$

Here the matrix M reads:

$$M = \begin{pmatrix} 0 & \Omega_p \psi_a^{0*} & 0 & 0 \\ \Omega_p \psi_a^0 & -[\Delta + i\gamma] & \Omega_{d1}/2 & \Omega_{d2}/2 \\ 0 & \Omega_{d1}/2 & 0 & 0 \\ 0 & \Omega_{d2}/2 & 0 & 0 \end{pmatrix}. \quad (75)$$

Note that this matrix is very similar to the Hamiltonian (25) for the linear tripod. The main difference between them is dependence of M on ψ_a^0 , that arises due to the nonlinearity. On the other hand, this matrix is also similar with corresponding matrix for the nonlinear lambda system. The Jacobian of the linearized system is given by $A = -iM$. The eigenvalues ω of the matrix M correspond to eigenvalues $\lambda = -i\omega$ of Jacobian. Solving the eigenvalues problem for matrix M , we get two zero eigenvalues:

$$\omega_{1,2} = 0. \quad (76)$$

The other two eigenvalues can be found from the quadratic equation

$$\omega^2 + (\Delta + i\gamma)\omega - (\Omega_{d1}^2 + \Omega_{d2}^2 + 4\Omega_p^2 |\psi_a^0|^2)/4 = 0. \quad (77)$$

The eigenvalues $\omega_{3,4}$ satisfy the condition

$$\omega_3 + \omega_4 = -[\Delta + i\gamma], \quad (78a)$$

$$\omega_3 \omega_4 = -[\Omega_{d1}^2 + \Omega_{d2}^2 + 4\Omega_p^2 |\psi_a^0|^2]/4. \quad (78b)$$

We again assume that $\Delta = 0$, thus obtaining the following solutions:

$$\omega_{3,4} = (-i\gamma \pm [-\gamma^2 + (\Omega_{d1}^2 + \Omega_{d2}^2 + 4\Omega_p^2 |\psi_a^0|^2)]^{1/2})/2. \quad (79)$$

Exactly as in the case of linear tripod, for $t \rightarrow \pm\infty$ the Rabi frequencies are zeros, and we get from (78) $\omega_3 = 0$ and $\omega_4 = -i\gamma$ thus yielding

$$\lambda_{1,2,3} = 0, \quad \lambda_4 = -\gamma. \quad (80)$$

In some range of time, $t_1 < t < t_2$, the discriminant is positive ($D \equiv -\gamma^2 + \Omega_{d1}^2 + \Omega_{d2}^2 + 4\Omega_p^2 |\psi_a^0|^2 > 0$). In this range we have

$$\omega_{3,4} = -i\gamma/2 \pm \sqrt{D}/2, \quad (81a)$$

$$\lambda_{3,4} = -\gamma/2 \mp i\sqrt{D}/2. \quad (81b)$$

The first two eigenvalues are $\lambda_{1,2} = \omega_{1,2} = 0$. The boundaries t_1, t_2 are the solutions of $D(t) = 0$ in respect to time. We thus have $\text{Re}(\lambda_{1,2}) = 0$ and $\text{Re}(\lambda_{3,4}) = -\gamma/2$ for $t_1 < t < t_2$.

As in the previous sections, we will plot the dynamics of the real parts of eigenvalues, i.e. $\text{Re}(\lambda) = \text{Re}(\lambda(t))$. The matrix M in the present case depends on ψ_a^0 , (see M_{ae} and M_{ea} in Eq.(75)). In the case of nonlinear

lambda system, the dark state was uniquely defined as a function of Rabi frequencies, Eq.(55). However, in the present case, for nonlinear tripod, the dark state is a manifold that is given by Eqs.(73). But we need a definite function of time $\psi_a^0 = \psi_a^0(t)$ in order to get the dynamics of eigenvalues. Therefore we use the parametrization of the dark state that was derived in Ref.[32]. If the solution of (71) evolves on the dark state manifold, we may express that solution in terms of only two variables (parameters), $[u_1(t), u_2(t)]$:

$$\psi_a^0 = \left[\frac{\delta_p}{\cos(\Theta)} \right]^{1/2} u_2^{1/2}, \quad (82a)$$

$$\psi_{g1}^0 = u_1 \sin(\Theta) - u_2 \cos(\Theta), \quad (82b)$$

$$\psi_{g2}^0 = -u_1 \cos(\Theta) - u_2 \sin(\Theta). \quad (82c)$$

(See the system of equations before Eqs.(17) in [32]). Here $\delta_p = \Omega_{d1}/\Omega_p$ and Θ is defined by $\tan(\Theta) = \Omega_{d2}/\Omega_{d1}$. In Ref.[32] it was also shown that in the adiabatic limit, the parameters should obey the equations (see Eqs.(17) in [32])

$$\dot{u}_1 + \dot{\Theta} u_2 = 0, \quad (83a)$$

$$\dot{u}_2 \left(1 + \frac{\delta_p}{4u_2 \cos(\Theta)} \right) - \dot{\Theta} u_1 + \frac{d}{dt} \left[\frac{\delta_p}{4 \cos(\Theta)} \right] = 0. \quad (83b)$$

We integrate the system (83) and insert its solution in the parametrization (82) thus obtaining the necessary dynamics of $\psi_a^0(t)$. After inserting this dynamics in (79) we get the dynamics of eigenvalues of the Jacobian for the nonlinear tripod system.

We may also suppose that the deviation for the amplitude ψ_a is almost zero, $\delta\psi_a(t) \simeq 0$. We thus can make a substitution in Eqs.(78) and (79):

$$\psi_a^0 \rightarrow \psi_a. \quad (84)$$

Subsequently one can numerically solve the system (71). By inserting $\psi_a(t)$ in (78) and (79), one gets the approximate dynamics of the eigenvalues. Actually, this approach means the analysis of the stability of the current solution $\Psi(t) = [\psi_a(t), \psi_e(t), \psi_{g1}(t), \psi_{g2}(t)]^T$. The dynamics of $|\dot{\psi}_e(t)|$ and $|\dot{\psi}_e(t)|^2$ is plotted in Fig.8(a). The first dynamics indicates that the magnitude of the r.h.s. of Eq.(71b) is of the order of 0.06. The second dynamics shows that the excited level remains almost unpopulated throughout the passage. We therefore conclude that the process is almost adiabatic, and one may justify the substitution (84).

In Fig.8(b) we plot the dynamics of $\text{Re}(\lambda(t))$ computed by the both ways. The black line shows the dynamics of $\text{Re}(\lambda(t))$ computed by using the exact value of $\psi_a^0(t)$, and the red line displays the approximate dynamics that is obtained by using the substitution (84). We can see from Fig.8(b) that the stability of the current solution (red line) is identical to that of the dark state at the

beginning and the middle of the process. However, the splitting of the real parts for the approximate eigenvalues is slightly delayed with respect to the exact ones. The good quantitative agreement of the both results confirms the validity of the approximation (84); it also shows that the current solution evolves in the close neighborhood of the moving dark state (82).

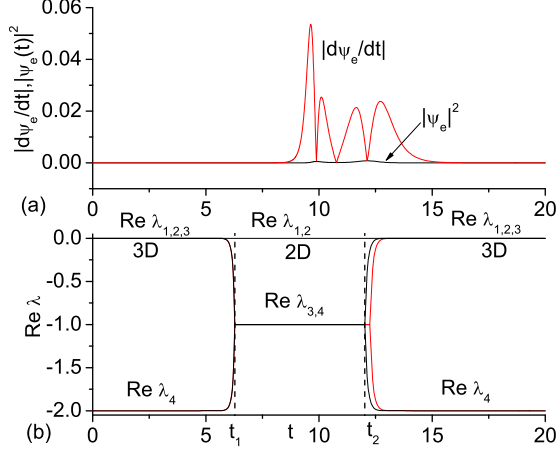


FIG. 8. (Color online) (a) Dynamics of $|\dot{\psi}_e(t)|$ (red), and $|\psi_e(t)|^2$ (black) for nonlinear tripod, both computed by (71); (b) dynamics of real parts of eigenvalues of the Jacobian for nonlinear tripod, computed by (79), and (76). The dashed black vertical lines set the boundaries for the 3D and 2D processes. Here $t_1 = 6.28$ and $t_2 = 12.02$. The parameters are as follows: $\Delta = 0$, $\gamma = 2.0$, $\Omega_0 = 60.0$, $t_p = 10.7$, $t_{d1} = 10.0$, $t_{d2} = 8.5$, $K_1 = 0.75$, $K_2 = 5.0$. The initial conditions are $\psi_a(0) = 1$, $\psi_{g1}(0) = \psi_{g2}(0) = \psi_e(0) = 0$.

Exactly as in the previous sections, we adiabatically eliminate the excited state by setting $\dot{\psi}_e = 0$. From Eq.(71b) we get

$$\psi_e = \frac{1}{2(\Delta + i\gamma)} (\Omega_p \psi_a^2 + \Omega_{d1} \psi_{g1} + \Omega_{d2} \psi_{g2}). \quad (85)$$

Inserting this expression in (71), we obtain

$$i\dot{\psi}_a = \Omega_p \psi_a^* \psi_e, \quad (86a)$$

$$i\dot{\psi}_{g1} = \frac{1}{2} \Omega_{d1} \psi_e, \quad (86b)$$

$$i\dot{\psi}_{g2} = \frac{1}{2} \Omega_{d2} \psi_e. \quad (86c)$$

In these equations we use the expression of ψ_e given by (85).

In Fig.9 we have plotted the dynamics for the case of nonlinear tripod. Figure 9(a) shows a sequence of Gaussian pulses. In Fig.9(b) we show the dynamics of populations of the levels. The solutions of approximated system are in good quantitative agreement with those of the exact system. From Fig.9(c) we see that the population of the excited state is reproduced by the approximated system with a significant error. Again, as in the previous section, we explain this fact by small magnitude

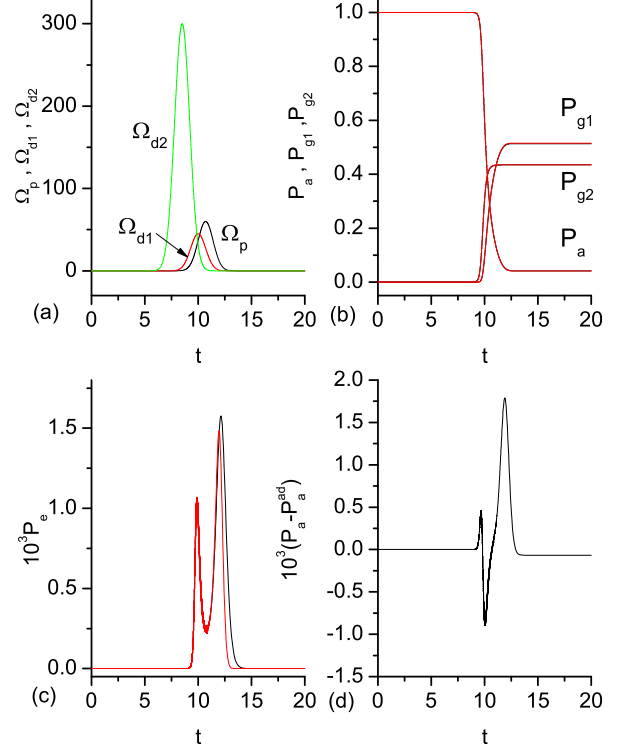


FIG. 9. (Color online) The dynamics (a) of Gaussian pulses (24), (b) of populations P_a, P_{g1}, P_{g2} , and (c) of population P_e in enlarged scale. In (d) it is shown the difference between the exact (P_a from Eqs.(71)) and adiabatically approximated (P_a^{ad} from Eqs.(86)) populations in enlarged scale. In (b,c) the black lines represent the solutions of exact Eqs.(71), and the red lines are the solutions of adiabatically approximated system (86) with excited state given by (85). The parameters are as follows: $\Delta = 0$, $\gamma = 2.0$, $\Omega_0 = 60.0$, $t_p = 11.5$, $t_{d1} = 10.0$, $t_{d2} = 8.5$, $K_1 = 0.75$, $K_2 = 5.0$. The initial conditions are the same as in Fig.8.

of quantity P_e . In Fig.9(d) we have plotted the difference between exact (P_a) and adiabatically approximated (P_a^{ad}) population P_a . It is of the same order as in the case of excited state (see Fig.9(c)).

VI. SOME REMARKS ABOUT THE ONE-PHOTON DETUNING

Up to now we have been setting $\Delta = 0$ for all considered systems. In this Section we shall explore a behavior of the system in the presence of the non-zero one-photon detuning $\Delta \neq 0$. In that case, when solving the quadratic equations for the eigenvalues of the Jacobians, one gets the complex-valued discriminants, $D \equiv |D|e^{i\varphi}$, where $|D|$ is their real amplitude, and φ is their phase. The

eigenvalues of the Jacobian then read:

$$\lambda_{3,4} = \left[-\frac{1}{2}\gamma \pm \frac{1}{2}|D|^{1/2} \sin\left(\frac{\varphi}{2}\right) \right] + i \left[\frac{1}{2}\Delta \mp \frac{1}{2}|D|^{1/2} \cos\left(\frac{\varphi}{2}\right) \right]. \quad (87)$$

Here the real and imaginary parts of the discriminant are given by

$$\text{Re}(D) = \Delta^2 - \gamma^2 + \Omega_{d1}^2 + \Omega_{d2}^2 + 4\Omega_p^2 |\psi_a^0|^2, \quad (88a)$$

$$\text{Im}(D) = 2\gamma\Delta. \quad (88b)$$

These equations are valid for the nonlinear tripod; for the other systems we get the similar expressions. If $\Delta = 0$ (as assumed previously), the imaginary part becomes zero, i.e. $\text{Im}(D) = 0$; the phase may be either 0 or π ; in the interval $t_1 < t < t_2$, it is $\varphi = 0$, and in the ranges $t < t_1$, $t > t_2$ it is $\varphi = \pi$. For $\varphi = 0$ we have $\text{Re}(\lambda_{3,4}) = -\gamma/2$, and for $\varphi = \pi$ we get $\text{Re}(\lambda_3) \simeq 0$, $\text{Re}(\lambda_4) \simeq -\gamma$. We have got these results for all the considered systems (see e.g. Fig.8(b)). However, in the case of the non-zero one-photon detunings, in the interval $t_1 < t < t_2$, these real parts are no longer coinciding; they are symmetrically surrounding the value $-\gamma/2$, and the difference between them becomes equal to

$$\begin{aligned} \text{Re}\lambda_3 - \text{Re}\lambda_4 &= |D|^{1/2} \sin\left(\frac{\varphi}{2}\right) \simeq \\ &\simeq \frac{\text{Im}(D)}{2[\text{Re}(D)]^{1/2}}. \end{aligned} \quad (89)$$

The latter approximation is valid for the small values of $\text{Im}(D) \ll \text{Re}(D)$. Such a situation takes place in the middle of the passage, when the Rabi frequencies are large compared to the one-photon detuning and losses.

We thus conclude that for such small detunings the difference between the negative real parts remains small, and our statements about the reduction of dimension remain valid.

VII. CONCLUSIONS

We have developed a systematic approach for adiabatic reduction of dimension of the linear and nonlinear three- and four-level systems. By evaluating the corresponding Jacobians and computing the dynamics of real parts of their eigenvalues (the non-zero eigenvalues are found from quadratic characteristic equations), one may define the dimensionality of the processes. This dimensionality is given by the number of zero real parts since the negative real parts cause the contraction of the nearby solutions towards the dark state. At the beginning and the end of the dynamics, there is always only one negative real part. Hence one may eliminate only one state representing the excited state. In the middle of the process, one of the zero real parts becomes negative thus making the number of negative real parts equal to two. In this

time interval we may eliminate two variables corresponding to excited and bright state respectively. For the linear systems, we eliminated both excited and bright states. However, for nonlinear systems, we have restricted ourselves by eliminating the excited state. This is due to the fact that the definition of a bright state for the nonlinear systems is not available.

A sensitive problem is the definition of a dark state for the nonlinear tripod. In the case of nonlinear lambda system, the dark state is a moving point (55) in the phase space. However, for the nonlinear tripod we have a manifold (73) of dark states. If one wishes to get the dynamics of real parts of eigenvalues of the Jacobian, one needs a definite value of complex amplitude ψ_a^0 belonging to the manifold. We here use two ways for the stability analysis of the dark state. The first way is to parametrize the dark state manifold by using the method developed in Ref.[32]. This method enables one to find the definite dynamics of $\psi_a^0(t)$. We thus managed to find the exact dynamics of eigenvalues. The second way is to simply substitute using Eq.(84) the value $\psi_a^0(t)$ by the current solution $\psi_a(t)$ that is found from underlying equations (71). Actually, the substitution (84) means we are investigating the stability of the current solution instead of that for the dark state. In fact, Fig.8(b) shows that the real parts of the eigenvalues evolve almost identically. The only difference is that the splitting of real parts for approximate eigenvalues is slightly delayed. Such a coincidence shows that the current solution evolves in the close neighborhood to the motion of the parametrized dark state (82). It is also to be noted that the magnitude of $|\dot{\psi}_e|$ is always small, and the excited state remains almost unpopulated as we can see in Fig.8(a).

It is noteworthy that a related approach was used in Ref.[30], where a feedback control scheme was presented that designs time-dependent laser-detuning frequency to suppress possible dynamical instability in coupled free-quasibound-bound atom-molecule condensate systems. It was proposed to perform a substitution analogous to (84) which was used for solving the control problem. On the other hand in our work this substitution was made for the stability analysis of the dark state.

It is also important to note that in the lambda and tripod systems, we have phenomenologically included the loss coefficient γ . This was done by making the one-photon detuning to be a complex number, i.e. by replacing $\Delta \rightarrow \Delta + i\gamma$. Here Δ is again a one-photon detuning, and γ determines the losses. In our work, we have considered the cases where $\Delta = 0$ and $\gamma > 0$, i.e. the one-photon resonances with losses. We stress that the presence of non-zero losses γ makes the adiabatic approximation easier to implement. The losses cause the appearance of two negative real parts of eigenvalues of the corresponding Jacobians. On the other hand, it was shown that the losses decrease the transfer efficiency [8], which decreases exponentially with the (small) decay rate. However the range of decay rates, over which the transfer efficiency remains high, appears to be pro-

portional to the squared pulse area. Hence, by choosing high pulse areas one may preserve the high transfer efficiency.

Another question is a possible presence of the one-photon detuning in the considered processes. As it was shown in Sec. VI, the relatively small one-photon detuning does not alter our conclusions about the reduction of dimension in the three- and four-level systems considered here. This happens if the Rabi frequencies are large compared to the one-photon detuning and loss rates.

We should also note that the range of validity for the 1D (2D) reduced system for lambda systems (for tripods) may be slightly larger than the time interval $t_1 < t < t_2$ (here t_1, t_2 correspond to the zeros of the discriminants involved in quadratic characteristic equations). For example, in Fig. 5 we see that 2D reduced linear tripod equations are valid in the time range $t \in [3.0, 13.0]$ whereas the discriminant is positive in the

range $(t_1, t_2) = (6.12, 12.73)$. Such a situation takes place because at $t < t_1$ there is a short transient process where one zero real eigenvalue ($\text{Re}(\lambda_3)$) moves towards $-\gamma/2$, and the negative real eigenvalue ($\text{Re}(\lambda_4)$) also moves from $-\gamma$ to $-\gamma/2$. In this short range of time we have, strictly speaking, two real negative eigenvalues, although one of them is much smaller than the other. The transient period is relatively short and terminates when the Rabi frequencies entering the discriminant (D) (for linear tripod it is defined below Eq. (30)) are large enough. In a similar way one may explain the process taking place for a short transient period at $t > t_2$ where an inverse process happens.

VIII. ACKNOWLEDGEMENT

The authors acknowledge the support by the EU FP7 project STREP NAMEQUAM.

-
- [1] K. Bergmann, H. Theuer, and B. W. Shore, Rev. Mod. Phys. **70**, 1003 (1998).
 - [2] N. V. Vitanov, T. Halfmann, B. W. Shore, and K. Bergmann, Annu. Rev. Phys. Chem. **52**, 763 (2001).
 - [3] N. V. Vitanov, M. Fleischhauer, B. W. Shore, and K. Bergmann, Adv. At. Mol. Opt. Phys. **46**, 55 (2001).
 - [4] E. Arimondo, in *Progress in Optics, vol. 35*, edited by E. Wolf (Elsevier, 1996) p. 259.
 - [5] P. Kral, I. Thanapulos, and M. Shapiro, Rev. Mod. Phys. **79**, 53 (2007).
 - [6] J. Oreg, F. T. Hioe, and J. H. Eberley, Phys. Rev. A **29**, 690 (1984).
 - [7] C. E. Carrol and F. T. Hioe, J. Opt. Soc. Am. B **42**, 1335 (1988).
 - [8] N. V. Vitanov and S. Stenholm, Phys. Rev. A **56**, 1563 (1997).
 - [9] R. G. Unanyan, L. P. Yatsenko, K. Bergmann, and B. W. Shore, Opt. Commun. **139**, 48 (1997).
 - [10] P. A. Ivanov, N. V. Vitanov, and K. Bergmann, Phys. Rev. A **70**, 063409 (2004).
 - [11] P. A. Ivanov, N. V. Vitanov, and K. Bergmann, Phys. Rev. A **72**, 053412 (2005).
 - [12] G. S. Vasilev, A. Kuhn, and N. V. Vitanov, Phys. Rev. A **80**, 013417 (2009).
 - [13] R. Unanyan, M. Fleischhauer, B. W. Shore, and K. Bergmann, Opt. Commun. **155**, 144 (1998).
 - [14] R. G. Unanyan, B. W. Shore, and K. Bergmann, Phys. Rev. A **59**, 2910 (1999).
 - [15] C. Lazarou and N. V. Vitanov, Phys. Rev. A **82**, 033437 (2010).
 - [16] H. Theuer, R. G. Unanyan, C. Habscheid, K. Klein, and K. Bergmann, Opt. Expr. **4**, 77 (1999).
 - [17] H. Goto and K. Ichimura, Phys. Rev. A **75**, 033404 (2007).
 - [18] Z. Kis, N. V. Vitanov, A. Karpati, C. Barthel, and K. Bergman, Phys. Rev. A **72**, 033403 (2005).
 - [19] R. Garcia-Fernandez, B. W. Shore, K. Bergmann, A. Ekers, and L. P. Yatsenko, J. Chem. Phys. **125**, 014301 (2006).
 - [20] K. Winkler, G. Thalhammer, M. Theis, H. Ritsch, R. Grimm, and J. H. Denschlag, Phys. Rev. Lett. **95**, 063202 (2005).
 - [21] S. Moal, M. Portier, J. Kim, J. Dugue, U. D. Rapol, M. Leduc, and C. C. Tanoudji, Phys. Rev. Lett. **96**, 023203 (2006).
 - [22] H. Y. Ling, H. Pu, and B. Seaman, Phys. Rev. Lett. **93**, 250403 (2004).
 - [23] H. Pu, P. Maenner, W. Zhang, and H. Y. Ling, Phys. Rev. Lett. **98**, 050406 (2007).
 - [24] H. Y. Ling, P. Maenner, W. Zhang, and H. Pu, Phys. Rev. A **75**, 033615 (2007).
 - [25] A. P. Itin and S. Watanabe, Phys. Rev. Lett. **99**, 223903 (2007).
 - [26] A. P. Itin, S. Watanabe, and V. V. Konotop, Phys. Rev. A **77**, 043610 (2008).
 - [27] J. J. Hope, M. K. Olsen, and L. I. Plimak, Phys. Rev. A **63**, 043603 (2001).
 - [28] S. Y. Meng, L. B. Fu, and J. Liu, Phys. Rev. A **78**, 053410 (2008).
 - [29] M. Mackie, R. Kowalski, and J. Javanainen, Phys. Rev. Lett. **84**, 3803 (2000).
 - [30] J. Cheng, S. Han, and Y. Yan, Phys. Rev. A **73**, 035601 (2006).
 - [31] C. Zhao, X. B. Zou, H. Pu, and G. C. Guo, Phys. Rev. Lett. **101**, 010401 (2008).
 - [32] X. F. Zhou, Y. S. Zhang, Z. W. Zhou, and G. C. Guo, Phys. Rev. A **81**, 043614 (2010).
 - [33] J. H. Wu, C. L. Cui, N. Ba, Q. R. Ma, and J. Y. Gao, Phys. Rev. A **75**, 043819 (2007).
 - [34] J. Liu, B. Wu, H. Pu, and Q. Niu, Phys. Rev. Lett. **90**, 170404 (2003).
 - [35] H. Jing, J. Cheng, and P. Meystre, Phys. Rev. Lett. **99**, 133002 (2007).
 - [36] H. Jing and Y. Jiang, Phys. Rev. A **77**, 065601 (2008).
 - [37] H. Jing, J. Cheng, and P. Meystre, Phys. Rev. A **77**, 043614 (2008).
 - [38] H. Jing, F. Zheng, Y. Jiang, and Z. Geng, Phys. Rev. A **78**, 033617 (2008).

- [39] K. Eckert, M. Lewenstein, R. Corbalan, G. Birkel, W. Ertmer, and J. Mompart, Phys. Rev. A **70**, 023606 (2004).
- [40] E. Pazy, I. Tikhonenkov, I. B. Band, M. Fleischhauer, and A. Vardi, Phys. Rev. Lett. **95**, 170403 (2005).
- [41] J. Larson, arxiv:1105.2731 (2011).
- [42] H. Jing, Y. Deng, and P. Meystre, Phys. Rev. A **83**, 063605 (2011).
- [43] X. F. Zhang, J. C. Chen, B. Li, L. Wen, and W. M. Liu, arxiv:1108.5000 (2011).
- [44] S. Y. Meng, L. B. Fu, J. Chen, and J. Liu, Phys. Rev. A **79**, 063415 (2009).
- [45] S. S. Ivanov and N. V. Vitanov, arxiv:1106.0272 (2011).
- [46] H. Haken, *Synergetics* (ISBN 3-540-40824-X Springer-Verlag Berlin Heidelberg New York, 1983).
- [47] M. Mackie, A. Collin, and J. Javanainen, Phys. Rev. A **71**, 017601 (2005).